JOURNAL OF THERMOPHYSICS AND HEAT TRANSFER
Vol. 8, No. 4, Oct.–Dec. 1994

Dependent vs Independent Scattering in Fibrous Composites Containing Parallel Fibers

Siu-Chun Lee*
Applied Sciences Laboratory, Inc., Hacienda Heights, California 91745

The influence of fiber optical properties, size, and volume fraction on dependent scattering in fibrous media containing parallel fibers is investigated in this study. The extinction efficiency of a dense fibrous medium is obtained from a rigorous solution of Maxwell's relations by accounting for the near-field multiple scattering and far-field wave interference between closely spaced parallel fibers. The domains of dependent and independent scattering are demarcated by conducting a systematic analysis of the extinction efficiency as a function of the complex index of refraction ($m = n - ik$), size, and volume fraction of fibers. For the range of parameters considered, it is shown that the scattering regimes boundary is roughly independent of the index of refraction for nonabsorbing fibers ($k = 0$). If the fibers are absorbing ($k > 0$) the domains of dependent and independent scattering vary with the refractive index n. Dependent scattering then becomes important at a lower volume fraction and smaller size parameter as n increases. The scattering regimes for nonabsorbing fibers also shows close agreement with those for nonabsorbing spheres.

Nomenclature

A = coefficient in the pair-correlation function
a = constant in the pair-correlation function
a_{jn} = dependent scattering wave coefficient, TE mode
${}^0a_{jn}$ = independent scattering wave coefficient, TE mode
b_{jn} = dependent scattering wave coefficient, TM mode
${}^0b_{jn}$ = independent scattering wave coefficient, TE mode
c_0 = constant, -1 or 1
d = diameter of fibers
$\boldsymbol{e}$ = unit vector
f_v = volume fraction of fibers, $\pi r_0^2 n_0 L_0$
f_{v0} = critical volume fraction demarcating the scattering regimes
$g(R)$ = pair-correlation function
H_n = Hankel function of the second kind
i = $\sqrt{-1}$
J_n = integral order Bessel function
K = complex effective propagation constant of fibrous medium
k = imaginary part of complex refractive index m, or index, 1 to N_0
k_0 = propagation constant of medium, $2\pi/\lambda$
L = $K \cos \phi_t$
L_0 = average fiber length
l_0 = $k_0 \cos \phi_i$
m = complex refractive index of fiber, $n - ik$
N_0 = total number of fibers
n = real part of complex refractive index, or index, $-\infty$ to ∞
n_0 = number of fibers per unit volume
Q_e = extinction efficiency
R = magnitude of $\boldsymbol{R}$
$\boldsymbol{R}$ = radial vector
R_{jk} = radial distance between fibers j and k
r_0 = radius of fiber
s = index, $-\infty$ to ∞
u = scalar potential function, TM mode
V = volume of medium
v = scalar potential function, TE mode
α = size parameters, $2\pi r_0/\lambda$
γ = polar angle
γ_{jk} = angle that the line joining the centers of fibers j and k makes with the X axis
δ_{jk}, δ_{ns} = Kronecker delta function
ε_j = phase shift of the primary incident wave at fiber j relative to the origin
θ = azimuthal angle, as shown in Fig. 1
λ = wavelength
T = transmittance
τ = optical depth
ϕ = polar angle, as shown in Fig. 1

Subscripts
d = refers to dependent scattering
e = extinction
i = refers to the incident wave
j, k = index, refers to the fiber
t = refers to the transmitted wave
0 = refers to independent scattering

Superscripts
I = TM mode
II = TE mode

Received Dec. 6, 1993; revision received May 2, 1994; accepted for publication May 9, 1994.

*Vice President, Mailing Address: P.O. Box 90333, Industry, CA 91715. Member AIAA.

Introduction

FIBROUS materials are widely utilized for thermal insulation in many commercial and aerospace systems due to their effectiveness in suppressing radiation. It has been established that radiation constitutes a significant portion of the total heat heat transfer through fibrous insulations, even at atmospheric conditions.[1-3] Therefore, reduction of radiant transfer is critical to improving the thermal insulation capacity of fibrous materials. Common fibrous insulations include high-porosity media, such as building insulations and Space Shuttle thermal protection tile materials, and high-density media such as the woven fabric or filament wound insulations. Fibers in these thermal insulations are usually a few micrometers in diameter and several millimeters in length. While high-porosity fibrous materials generally consist of loosely filled, randomly oriented fibers, many high-density fibrous media such as the woven fabrics and ceramic fibrous composites consist of highly structured arrays of closely spaced parallel fibers. The radiative properties of these different types of fibrous media depend greatly on the concentration and orientation of fibers in the matrix.

Before proceeding with the development of this article, it should be pointed out that we are concerned here with infinite fibers whose radii r_0 are comparable to wavelength λ. The assumption of infinite fibers is easily satisfied by fibers in fibrous insulations, which are usually a few microns in diameter and several millimeters long. We refer to a high-porosity medium as one in which the separation between fiber centers c is much greater than λ (i.e., $r_0 \sim \lambda$, $c >> \lambda$), and a high-density medium if the fiber separation is comparable to λ (i.e., $r_0 \sim \lambda$, $c \sim \lambda$). A brief discussion of the terminology "dependent scattering" is also given here. In the study of wave propagation, scattering is generally regarded as either coherent or incoherent. Technically, coherent scattering refers to the condition where scattered light has the same frequency as the incident light. However, coherent scattering is often used with a connotation associated with incoherent scattering, such that it refers to the condition in which definite relationships exist between the phases and amplitudes of the scattered waves from all the scatterers in the medium, i.e., correlated scattering. Coherent scattering generally occurs in a high-density medium containing closely spaced scatterers. On the other hand, if the scatterers are far apart as in a high-porosity medium, there is no definite relationship between the amplitudes and phases of the scattered waves arising from the different scatterers. Scattering is incoherent or uncorrelated, and the addition rule holds for the radiative properties of the scatterer medium. The total scattered intensity at a point in space is simply equal to the sum of those contributed by all the scatterers. In summary, dependent scattering generally refers to the case in which scattering is correlated, whereas uncorrelated scattering is commonly called independent scattering (e.g., Refs. 4 and 5, and the references cited therein). In this article, for no other reason than to follow tradition, dependent and independent scattering are used to designate scattering phenomena pertaining to coherent and incoherent scattering, respectively.

The analysis of radiative transfer through high-porosity fibrous media is relatively straightforward due to the assumption of independent scattering, for which the radiative transfer equation (RTE) is employed. The radiative properties of fibers are based on the scattering of electromagnetic (EM) waves by an isolated cylinder.[6] Earlier radiative analyses on fibrous media considered only fibers that are randomly oriented in space.[7,8] Radiant transport models for fibrous media with arbitrary fiber orientations were later developed by accounting for the influence of fiber orientation.[9,10] For high-density fibrous materials, the analysis of radiative properties is complicated by the dependent scattering effects (i.e., near-field multiple scattering and far-field wave interference).[11] Thus far, theoretical formulations on the radiative properties of closely spaced fibers are available only for parallel fibers, such as those in woven fabric insulations and ceramic fibrous composites. A survey of the radiative modeling to-date of finite collection and dense medium of closely spaced parallel fibers is given below.

Based on a rigorous consideration of EM theory, Olaofe[12] presented the multiple scattering formalism for a finite collection of closely spaced, parallel infinite cylinders at normal incidence. By accounting for the depolarization of the scattered waves at oblique incidence, Lee generalized the scattering formalism for arbitrary incidence on homogeneous[13] and radially stratified cylinders.[14] These finite configuration formalisms can, in principle, be applied to predict the radiative properties of a high-density fibrous medium by specifying the location of each of the fibers in the medium. This brute-force approach is obviously impractical for a dense medium containing numerous fibers due to the extremely large demand on computer memory and excessive computer execution time. Therefore, a statistical approach must be applied to evaluate the radiative propagation characteristics through dense fibrous media.

Earlier formulations on the effective propagation constant of dense fibrous media include those by Bose and Mal[15] and Varadan et al.[16] for acoustic and elastic waves at normal incidence to homogeneous, infinite parallel cylinders. These formulations are equally applicable to radiant energy transport because the propagation of acoustic, elastic, and EM waves is all governed by the Helmholtz equation. By accounting for the decomposition of polarization, the general formulations for oblique incidence on dense fibrous media containing bare and coated fibers were developed by Lee.[17,18] The formulations reported in Refs. 15–18 are applicable to fiber sizes comparable to the wavelength and for arbitrary complex refractive index (with appropriate transformation of the elastic constants in Refs. 15 and 16 to the dielectric properties). By considering only the far-field wave interference effect based on the Rayleigh-Gans (R-G) theory, approximate formulas for scattering properties were reported by White and Kumar[19] and Kumar and White[20] for parallel fibers at normal incidence. The R-G theory assumes a negligible deviation of m from that of the surrounding medium, i.e., $|m - 1| << 1$ for fibers in free space, and that the phase shift of the EM wave traversing the fibers must be negligible, i.e., $2\alpha|m - 1| << 1$.[4] These conditions are rarely satisfied for real fibrous materials in the thermal radiation regime, since the refractive index of fibers is usually complex and the fiber diameter is comparable to the wavelength. The contribution of the near- and far-field effects to the radiative properties of closely spaced fibers was examined in a recent study,[21] which revealed that neglecting the near-field interactions for fibers of moderate size parameter would lead to the nonphysical result of a negative absorption coefficient.

With the advent of woven fabric insulations and ceramic fibrous composites for high-temperature applications, accurate radiative heat transfer analyses are needed to develop optimal designs and predict the performance. Therefore, it is necessary to understand the effect of fiber size and optical properties on the radiative properties of a fibrous medium as the fiber volume fraction increases. The objective of this study is to examine the conditions for which dependent scattering would become important for fibrous media containing parallel fibers. This is achieved by a systematic analysis of the radiative propagation characteristics in a fibrous medium. This article will begin with a discussion of the theoretical basis.

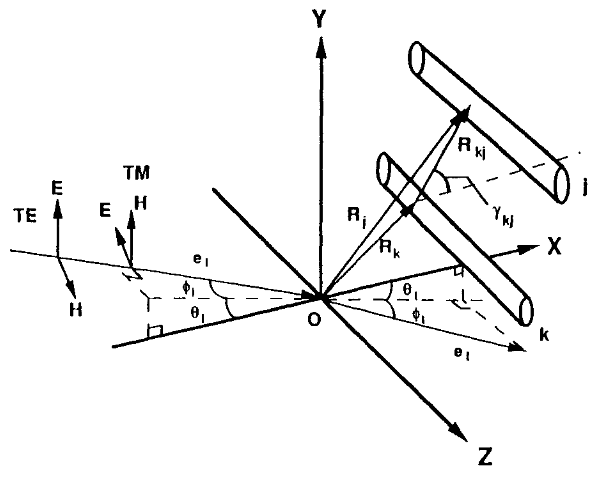

Fig. 1 Plane EM wave at oblique incidence on a dense medium of fibers.

Theory

It is well established that the radiative properties of a high-porosity, i.e., independent, scattering medium are equal to the sum of those for the isolated scatterers.[4] In a high-density medium (r_0, $c \sim \lambda$), this simple addition rule is no longer valid due to dependent scattering in the near and far fields. The formal solution including the dependent scattering effects in a dense fibrous medium must be obtained by solving Maxwell's equations. Detailed formulations of radiative propagation through a medium of closely spaced parallel fibers at oblique incidence have been presented by Lee.[13,14] For continuity, the formulations are briefly summarized here.

For a plane EM wave at oblique incidence on a collection of parallel fibers as shown in Fig. 1, the total scalar wave potentials at a point P in space with respect to fiber j are equal to the sum of the contributions of the scattered waves from all fibers. These potential functions correspond to the z component of the magnetic and electric hertz vectors, respectively, which satisfy the scalar Helmholtz equation. The total scalar potentials including depolarization at oblique incidence are summarized as[13]

$$u_j(\boldsymbol{R}_p) = u_j^0(\boldsymbol{R}_p) + c_0 \sum_{n=-\infty}^{\infty} (-1)^n \exp(in\gamma_{jp}) \times \sum_{k=1}^{N_0} b_{kn} H_n(l_0 R_{kp}) \tag{1}$$

for the transverse magnetic (TM) mode incident wave, and

$$v_j(\boldsymbol{R}_p) = v_j^0(\boldsymbol{R}_p) - c_0 \sum_{n=-\infty}^{\infty} (-1)^n \exp(in\gamma_{jp}) \times \sum_{k=1}^{N_0} a_{kn} H_n(l_0 R_{kp}) \tag{2}$$

for the transverse electric (TE) mode incident wave. In the above expressions, N_0 is the total number of fibers, $\boldsymbol{R}_p$ is the radial vector to point P, $l_0 = k_0 \cos\phi_i$, k_0 is the propagation constant of the medium containing the fibers, H_n is the Hankel function of the second kind, and b_{kn} and a_{kn} are unknown coefficients. The superscripts I and II associated with u, v, b_{kn}, and a_{kn}, which denote the TM and TE mode, respectively, have been omitted for brevity. The potential functions of the incident wave are given by

$$u_j^0(\boldsymbol{R}_p) = \exp(-ik_0 \boldsymbol{e}_i \cdot \boldsymbol{R}_p), \quad v_j^0(\boldsymbol{R}_p) = 0, \quad c_0 = -1 \tag{3}$$

for an incident TM wave, and

$$v_j^0(\boldsymbol{R}_p) = \exp(-ik_0 \boldsymbol{e}_i \cdot \boldsymbol{R}_p), \quad u_j^0(\boldsymbol{R}_p) = 0, \quad c_0 = 1 \tag{4}$$

for an incident TE wave, where $\boldsymbol{e}_i$ is the unit vector in the direction of the incident wave. At oblique incidence both $u_j(\boldsymbol{R}_p)$ and $v_j(\boldsymbol{R}_p)$ exist due to the decomposition of polarization. By invoking the continuity of the tangential components of the electric and magnetic field vectors across the surface of each fiber, the following set of equations is obtained for the unknown wave coefficients of an incident TM wave:

$$\sum_{s=-\infty}^{\infty} \sum_{k=1}^{N_0} \{[\delta_{jk}\delta_{ns} + (1 - \delta_{jk}) G_{ks}^{jn}\, {}^0b_{jn}^{\mathrm{I}}] b_{jn}^{\mathrm{I}} + (1 - \delta_{jk}) G_{ks}^{jn}\, {}^0b_{jn}^{\mathrm{II}}] a_{jn}^{\mathrm{I}}\} = \varepsilon_j\, {}^0b_{jn}^{\mathrm{I}} \tag{5}$$

$$\sum_{s=-\infty}^{\infty} \sum_{k=1}^{N_0} \{[\delta_{jk}\delta_{ns} + (1 - \delta_{jk}) G_{ks}^{jn}\, {}^0a_{jn}^{\mathrm{II}}] a_{jn}^{\mathrm{I}} + (1 - \delta_{jk}) G_{ks}^{jn}\, {}^0a_{jn}^{\mathrm{I}}] b_{jn}^{\mathrm{I}}\} = \varepsilon_j\, {}^0a_{jn}^{\mathrm{I}} \tag{6}$$

where $\varepsilon_j[=\exp(-ik_0 \boldsymbol{e}_i \cdot \boldsymbol{R}_j)]$ is the phase shift of the incident wave at fiber j

$$G_{ks}^{jn} = (-i)^{s-n} H_{s-n}(l_0 |\boldsymbol{R}_j - \boldsymbol{R}_k|) \exp[i(s-n)\gamma_{kj}] \tag{7}$$

and the wave coefficients with the upper-left superscript 0 refer to those for scattering by an isolated fiber. The corresponding expressions for a TE mode incident wave are obtained by making the following substitutions: $b_{jn}^{\mathrm{I}} \to b_{jn}^{\mathrm{II}}$ and $a_{jn}^{\mathrm{I}} \to a_{jn}^{\mathrm{II}}$ in Eq. (5), $a_{jn}^{\mathrm{I}} \to a_{jn}^{\mathrm{II}}$ and $b_{jn}^{\mathrm{I}} \to b_{jn}^{\mathrm{II}}$ in Eq. (6), as well as ${}^0b_{jn}^{\mathrm{I}} \to {}^0b_{jn}^{\mathrm{II}}$ and ${}^0a_{jn}^{\mathrm{I}} \to {}^0a_{jn}^{\mathrm{II}}$ on the right side of Eqs. (5) and (6), respectively. By specifying the location of each of the fibers, Eqs. (5) and (6) can be solved for the wave coefficients that can then be used to obtain the total extinction and scattering cross sections of the finite collection of fibers.

As N_0 and V become very large, while $n_0(=N_0/V)$ remains finite, the average wave traverses the medium with K, which is different from k_0.[22] By utilizing ensemble averages, the relation governing both the TM and TE mode propagation constants at oblique incidence is given by the following determinant for both bare and coated fibers[17,18]:

$$\begin{vmatrix} \delta_{ns} + n_0\,{}^0b_n^{\mathrm{I}} F_{sn} & n_0\,{}^0b_n^{\mathrm{II}} F_{sn} \\ n_0\,{}^0a_n^{\mathrm{I}} F_{sn} & \delta_{ns} + n_0\,{}^0a_n^{\mathrm{II}} F_{sn} \end{vmatrix} = 0 \tag{8}$$

which is a transcendental equation containing the unknowns K, ϕ_t, and θ_t. The parameters ϕ_t and θ_t are complex angles specifying the propagating direction of the transmitted wave in the medium. Because the propagation constants of a dense discrete random medium are analogous to the optical constants of a homogeneous medium, Eq. (8) is often called the dispersion relation for the composite medium.[16] However, it must not be confused with the dispersion relation based on semiconductor theory for crystalline solids. In Eq. (8) the quantity n_0F_{sn} is given by[17,18]

$$n_0F_{sn} = \left(\frac{2f_v}{r_0^2}\right) \frac{e^{i(n-s)\theta_t}}{k_0^2 - K^2} [2l_0 r_0 J_{s-n}(2Lr_0) H'_{s-n}(2l_0 r_0) - 2Lr_0 H_{s-n}(2l_0 r_0) J'_{s-n}(2Lr_0)] + 8f_v e^{i(n-s)\theta_t} \times \int_1^{\infty} J_{s-n}(2Lr_0 t) H_{s-n}(2l_0 r_0 t)\{g(t) - 1\} t \,\mathrm{d}t \tag{9}$$

where $f_v(=\pi r_0^2 n_0 L_0)$ is the fiber volume fraction, $L = K\cos\phi_t$, $g(t)$ is the fiber radial distribution function, $t(=R/2r_0)$ is the nondimensional radial distance, and the superscript $'$ denotes differentiation with respect to the argument. The complex angles are related to ϕ_i and θ_i, describing the incident direction by Snell's laws:

$$k_0 \cos\phi_i \sin\theta_i = K \cos\phi_t \sin\theta_t \tag{10}$$

$$k_0 \sin\phi_i = K \sin\phi_t \tag{11}$$

Equations (8–11) provide a complete system that can be solved for K, ϕ_t, and θ_t. It can be shown from Eqs. (10) and (11) that K is independent of θ_t.

Evaluation of the dispersion relation requires the pair-correlation function $g(R)$. For closely spaced parallel fibers, the $g(R)$ based on the Monte Carlo analysis of an isothermal-isobaric ensemble of hard disks[23] or an empirical exponential form[15] can be used. These functions can be approximated by

$$g(R) = 1 + A \exp\{-a[R/(2r_0)^p]\}, \qquad R \geq 2r_0 \tag{12}$$

The values $A = 900$, $a = 4.85$, and $p = 1$, based on an approximate fit of the numerical values of the correlation function presented in Ref. 23, are used in the present analysis.

The extinction efficiency of the medium, which accounts for the dependent scattering effects is related to K by[22]

$$Q_{ed} = -\frac{\pi\alpha}{f_v}\,\mathrm{Im}\left(\frac{K}{k_0}\right) \tag{13}$$

where Im refers to the imaginary part. The values of Q_{ed} and K for unpolarized radiation are simply equal to the average of those for the TM and TE modes.

Demarcation Criterion

Demarcation of the scattering regimes requires the application of a specific criterion that generally depends on the quantity of interest, such as transmission, reflection, or radiative heat transfer. While the scattering regimes for transmission analyses can be obtained by a consideration of the extinction coefficient only, radiative heat transfer presents a much more complicated problem, because it varies strongly with the temperature and emittance of the boundaries. Therefore, the scattering regimes can only be developed by considering all combinations of boundary temperature and emittance, in conjunction with the spectral optical properties of the fibers, as well as the fiber size, volume fraction, and thickness of the medium.

Although a thorough analysis exhausting the range of all variables is undoubtedly most rigorous, the problem also becomes practically intractable due to the numerous combinations of the various parameters. A much less ambitious, albeit only approximate, approach is based on the consideration of the extinction efficiency. Because the extinction efficiency includes both absorption and scattering, it governs the attenuation of radiation, as well as the radiative transfer within the context of the diffusion approximation for an optically thick medium, which is usually the case for high-density fibrous media.

Consider the attenuation by a dense fibrous medium. The transmittance accounting for dependent scattering can be expressed as

$$\mathrm{T} = \exp(-\tau_{0d}) = \exp(-\tau_0 Q_{ed}/Q_{e0}) \tag{14}$$

where τ_0 is the optical depth based on the independent scattering extinction efficiency Q_{e0}. If dependent scattering is ignored in the analysis, the transmittance based on independent scattering would be calculated as

$$\mathrm{T}_0 = \exp(-\tau_0) \tag{15}$$

The ratio of the transmittance based on dependent and independent scattering is a function of $Q_{ed}/Q_{e0} - 1$, which measures the deviation of the effective extinction efficiency from the independent scattering value. Since the optical depth of a dense medium is usually very large due to the high fiber volume fraction, it is easy to see that even a 5% deviation of Q_{ed} from Q_{e0} would result in a rather substantial error if dependent scattering is neglected. Therefore, the deviation of Q_{ed}/Q_{e0} from unity is being used in the present study as the criterion to demarcate the scattering regimes.

Solution of Dispersion Relation

The extinction efficiency Q_{ed} of a fibrous medium is strongly influenced by the complex refractive index, size, and volume fraction of fibers, as well as the angle of incidence. Since EM waves propagating normal to the fiber axes traverse the shortest distance between successive scattering than at oblique incidence, near-field multiple scattering is more pronounced at normal incidence. Therefore, the subsequent analysis of scattering regimes is based on normal incidence for a conservative analysis.

At normal incidence the scattered waves do not become depolarized so that a TM/TE incident wave scatters as a TM/TE wave. The cross-mode coefficients ${}^0a_n^{\mathrm{I}}$ and ${}^0b_n^{\mathrm{II}}$ vanish, and Eq. (8) decomposes to

$$|\delta_{ns} + n_0{}^0b_n^{\mathrm{I}}F_{sn}| = 0 \tag{16}$$

$$|\delta_{ns} + n_0{}^0a_n^{\mathrm{II}}F_{sn}| = 0 \tag{17}$$

for the TM and TE modes, respectively. The roots of the complex analytic functions represented by these determinants are solved by utilizing the IMSL double precision subroutine DZANLY.[24]

Equations (16) and (17) are $(2N + 1) \times (2N + 1)$ determinants containing the unknown K, where N is the number of truncation terms. To minimize truncation errors, all calculations are performed in double precision. A solution K_0 is accepted only if both $|f_0(K_0)|$ and $|f_0(K_0)/(K - K_0)|$ are less than 1.E-5, where $f_0(K)$ is the complex analytic function. Values based on the Rayleigh limit formula[17] usually provide good initial guesses to start the iteration.

Analysis of Scattering Regimes

Extensive numerical analyses are performed to identify general trends for demarcating the scattering regimes. Instead of using the refractive index of a specific material, the real and imaginary parts of m are varied independently. The values of n and k used in the analyses are $n = 1.05$, 1.546, 2.0, 3.0, 4.0, and $k = 0.0$, 0.5, 1.0, which cover most materials of interest to thermal insulation applications. The size parameters are $\alpha = 0.01$, 0.05, 0.1, 0.5, 1, 2, and 17 volume fractions between 0.001–0.5 are used. Typical execution times to solve for the effective propagation constants on the 486/33 MHz PC for each combination of n and k for 17 values of f_v are 20 min for $\alpha = 0.01$, 1 h for $\alpha = 0.05$ and 0.1, 3 h for $\alpha = 0.5$, and in excess of 8 h for $\alpha = 1.0$. The increase in execution time with α is due to the larger number of terms that must be retained in the governing equations. Several values of K beyond $\alpha = 1.0$ are also obtained in order to assist the extrapolation to larger size parameters.

Typical variations of the efficiency ratio (Q_{ed}/Q_{e0}) with fiber volume fraction are shown in Figs. 2 and 3 for $\alpha = 0.05$ and 0.5, respectively, which reveal that Q_{ed}/Q_{e0} varies considerably with fiber optical properties. At very low volume fractions, Q_{ed}/Q_{e0} is nearly unity, indicating that independent scattering prevails. It then deviates from unity as the volume fraction increases due to the gradual importance of the dependent scattering effects. In order to demarcate the scattering regimes, the criterion of a 5% deviation of the efficiency ratio from unity is used. The volume fraction at which this occurs is designated as the critical volume fraction f_{v0} beyond which scattering becomes dependent. Based on this approach, maps of the scattering regimes are shown in Figs. 4 and 5 for

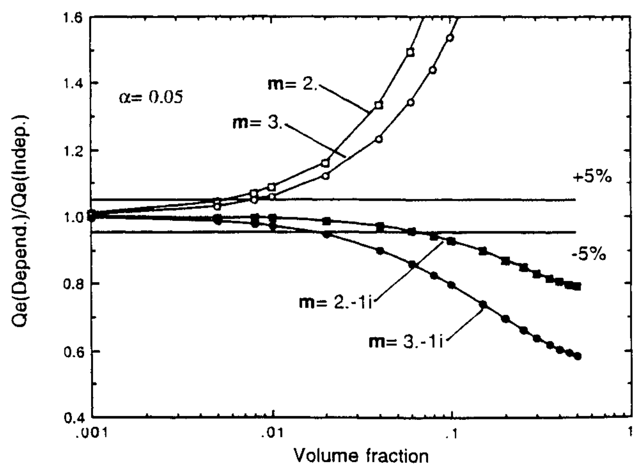

Fig. 2 Variation of the efficiency ratio with volume fraction for α = 0.05.

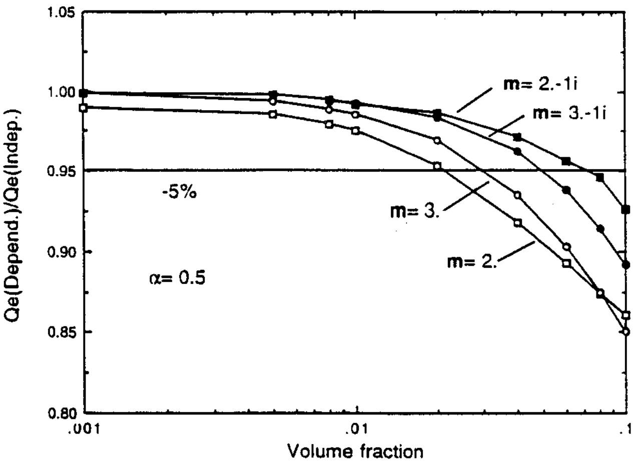

Fig. 3 Variation of the efficiency ratio with volume fraction for $\alpha = 0.5$.

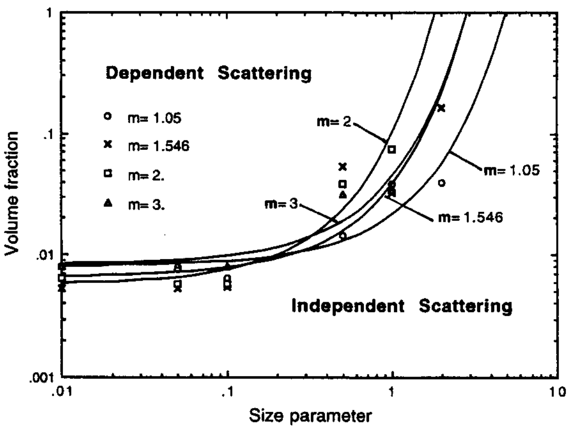

Fig. 4 Scattering regimes for real refractive index.

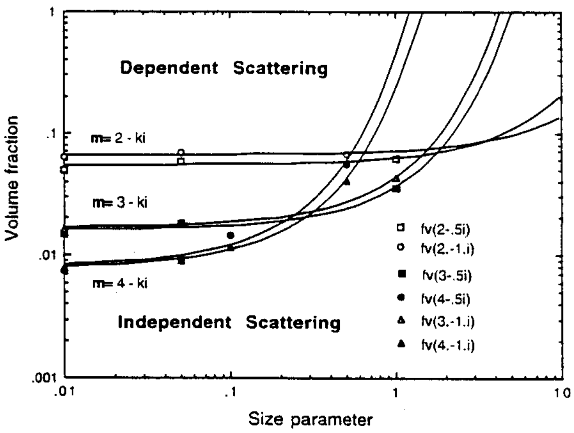

Fig. 5 Scattering regimes for complex refractive index.

nonabsorbing and absorbing fibers, respectively. A common feature of these results is that f_{v0} is relatively constant for $\alpha \leq 0.1$.

Figure 4 shows the critical volume fraction (f_{v0}) as a function of α for nonabsorbing fibers for $\alpha > 0.1$. Also shown are the curve-fits for the data of each refractive index, in which the region below the curves is the independent scattering regime. It is apparent from these data that an approximate boundary of the scattering regimes can be drawn for nonabsorbing fibers. In the case of absorbing fibers as shown in Fig. 5, the data for each complex index of refraction can be fitted similarly by the exponential form. These results reveal that absorption causes a shift of the scattering regimes, so that f_{v0} decreases as the real part of the complex refractive index increases. The size parameter beyond which dependent scattering is important also becomes smaller.

Approximate Model

For nonabsorbing fibers ($k = 0$), as shown in Fig. 4, the data set for each index of refraction can be fitted by expressions of the form $f_v = a_0 * 10 ** (b_0\alpha)$, where a_0 is approximately equal to the critical volume fraction f_{v0}. For m = 1.05, 1.546, 2, and 3, the constants are given by a_0 = 8.04E-03, 6.57E-03, 5.69E-03, and 8.25E-03; and b_0 = 0.417, 0.749, 1.22, and 0.716, respectively. It is apparent from Fig. 4 that all of the data can be represented approximately by a single expression. Based on the curve-fits for the various m, we obtain $f_v = f_{v0} * 10 ** (0.732\alpha)$ as an approximate fit for nonabsorbing fibers.

For absorbing fibers, i.e., $k > 0$, similar curve-fits can be obtained for the data. The trend of the curves is, however, quite distinct for each refractive index, as shown in Fig. 5. For a given refractive index n, only a small difference exists between the data for different absorption index k. As an approximation, therefore, a single curve-fit can be used for the data for the same n. The constants in the exponential analytic expressions are then given by f_{v0} = 5.98E-02, 1.86E-02, and 7.98; and b_0 = 4.48E-2, 0.418, and 1.57 for m = 2. − ki, 3. − ki, 4. − ki (k = 0.5, 1.0), respectively. To interpolate between $4 \geq n \geq 2$, we assume that the same variation of volume fraction with size parameter holds in this range. A third-order polynomial fit of b_0 with respect to n yields $b_0 = 1.633 - 1.573n + 0.389n^2$. Therefore, the expression for demarcating the scattering regimes for $4 \geq n \geq 2$ and $1 \geq k \geq 0.5$ is given by $f_v = f_{v0} * 10 ** [b_0(n)\alpha]$.

Based on the above results, a simple model for demarcating the scattering regimes can be derived. The model is based on two aspects. First, the critical volume fraction f_{v0} is relatively constant for $\alpha \leq 0.1$, which allows f_{v0} to be evaluated from the Rayleigh limit formulas. Second, the variation of f_{v0} with α is given by the curve-fits for $\alpha > 0.1$. This model is summarized below.

Region of $\alpha \leq 0.1$

The numerical results indicate that f_{v0} is relatively constant for size parameters less than 0.1. Therefore, f_{v0} can be determined from the analysis of Rayleigh limit fibers. In this limit the dispersion relations can be greatly simplified in the numerical evaluation of the effective propagation constant and extinction efficiency. In particular, only the leading terms in Eqs. (16) and (17) need to be retained, thus greatly expediting numerical computation. By calculating Q_{ed} as a function of f_v in the Rayleigh limit, the extinction ratio similar to those shown in Figs. 2 and 3 is generated. A 5% deviation of the extinction ratio from unity is then applied to yield

$$f_v = f_{v0} \tag{18}$$

as the boundary demarcating the scattering regimes for $\alpha \leq 0.1$.

Region $\alpha > 0.1$

The curve-fits on the data are applied in this region. For nonabsorbing fibers for $4 \geq n > 1.05$, the demarcation is identified by

$$f_v = f_{v0} * 10 ** (0.732\alpha) \tag{19}$$

where f_{v0} is the critical volume fraction given by Eq. (18). For absorbing fibers, the demarcation is given by

$$f_v = f_{v0} * 10 ** [(1.633 - 1.573n + 0.389n^2)\alpha] \tag{20}$$

for $4 \geq n \geq 2$ and $1 \geq k \geq 0.5$.

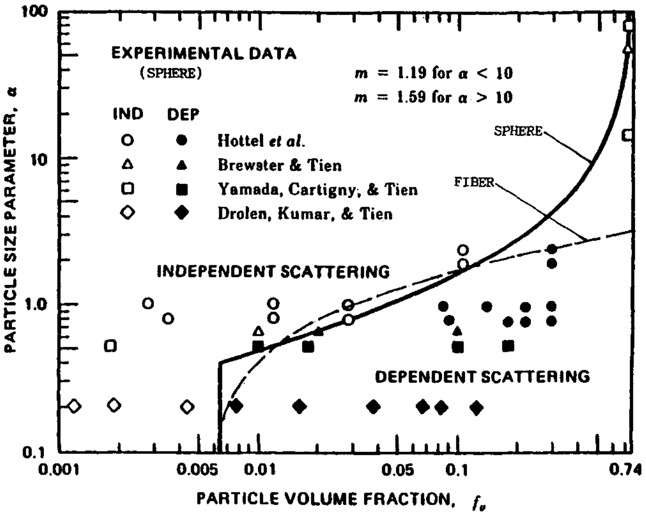

Fig. 6 Comparison of the scattering regimes for fibers and spheres.

A comparison is made between the present model for nonabsorbing fibers with the scattering regimes map for spheres, as shown in Fig. 6. The scattering regimes map for spheres as reported in Ref. 25 depicts a collection of test data for nonabsorbing spheres and a curve demarcating the domains of dependent and independent scattering. To obtain the corresponding map for fibrous media, the critical volume fraction f_{v0} is first calculated as described above for $\alpha \le 0.1$ and $m = 1.19$, which is the refractive index for the data on spheres. This yields $f_{v0} = 0.0052$, so that the demarcation curve is given by $f_v = 0.0052 * 10 ** (0.732\alpha)$. As shown in Fig. 6, the demarcation curve for fibrous media agrees well with the data for spheres. The good agreement is quite surprising in view of the considerable differences between the scattering behavior of fibers and spheres. Specifically, the scattered waves from spheres propagate as spherical waves that span the entire 4π-sr solid angle. The scattered waves from infinite fibers are cylindrical waves that are confined to propagate along the surface of a cone with an apex angle equal to $2\pi - \phi_i$, where ϕ_i is the angle of incidence. At normal incidence the cone opens up into a plane normal to the fiber axis.

Summary

Radiant energy transport in fibrous composites is strongly influenced by the size, optical properties, and f_v of fibers. Independent scattering generally prevails if $f_v << 1$, so that fibers scatter as isolated scatterers. As the fiber volume fraction increases, near-field multiple scattering and far-field wave interference gradually become dominant, and scattering would become correlated. Therefore, the adequacy of the independent scattering assumption must be assessed in the analysis of radiative transfer through a fibrous medium.

The present analysis of scattering regimes is based on theoretical formalisms that account for dependent scattering. The extinction efficiency Q_{ed} at normal incidence for a composite containing parallel fibers is obtained as a function of fiber volume fraction for a range of size parameter and complex refractive index. The deviation of Q_{ed} from the independent efficiency Q_{e0} as function of volume fraction reveals the gradual dominance of dependent scattering. A 5% deviation of Q_{ed}/Q_{e0} from unity is applied as the criterion for demarcating the scattering regimes.

The present results indicate that the scattering regimes are strongly affected by the complex index of refraction. For nonabsorbing fibers, a single demarcation curve is applicable for a refractive index between 1.05 and 4. For absorbing fibers ($1 \ge k \ge 0.5$), a family of curves is obtained for each refractive index ($n = 2, 3, 4$). These optical properties cover the range of many materials for thermal insulation applications. Finally, good agreement is observed between the present model for nonabsorbing fibers and the data for nonabsorbing spheres, despite the different scattering behavior of fibers and spheres.

References

[1]Verschoor, J. D., and Greebler, P., "Heat Transfer by Gas Conduction and Radiation in Fibrous Insulation," *Transactions of the American Society of Mechanical Engineers*, Vol. 74, No. 6, 1952, pp. 961–968.

[2]Bankvall, C. G., "Heat Transfer in Fibrous Materials," *Journal of Testing and Evaluation*, Vol. 1, No. 5, 1973, pp. 235–243.

[3]Pelanne, C. M., "Heat Flow Principles in Thermal Insulations," *Journal of Thermal Insulation*, Vol. 4, No. 1, 1980, pp. 27–44.

[4]Van de Hulst, H. C., *Light Scattering by Small Particles*, Dover, New York, 1981.

[5]Drolen, B. L., and Tien, C. L., "Thermal Radiation in Particulate Media with Dependent and Independent Scattering," *Annual Review of Numerical Fluid Mechanics and Heat Transfer*, Vol. 1, 1987, pp. 1–32.

[6]Lind, A. C., and Greenberg, J. M., "Electromagnetic Scattering for Obliquely Oriented Cylinders," *Journal of Applied Physics*, Vol. 37, No. 8, 1966, pp. 3195–3203.

[7]Houston, R. L., and Korpela, S. A., "Heat Transfer Through Fiberglass Insulation," *Proceedings of the 7th International Heat Transfer Conference*, Vol. 2, Hemisphere, Washington, DC, 1982, pp. 499–504.

[8]Tong. T. W., and Tien, C. L., "Radiative Transfer in Fibrous Insulations—Part 1: Analytical Study," *Journal of Heat Transfer*, Vol. 105, No. 1, 1983, pp. 70–75.

[9]Lee, S. C., "Effect of Fiber Orientation on Thermal Radiation in Fibrous Media," *International Journal of Heat and Mass Transfer*, Vol. 32, No. 2, 1989, pp. 311–319.

[10]Lee, S. C., "Scattering Phase Function for Fibrous Media," *International Journal of Heat and Mass Transfer*, Vol. 33, No. 10, 1990, pp. 2183–2190.

[11]Ishimaru, A., *Wave Propagation and Scattering in Random Media*, Vols. 1 and 2, Academic Press, New York, 1978.

[12]Oloafe, G. O., "Scattering by an Arbitrary Configuration of Parallel Circular Cylinders," *Journal of the Optical Society of America*, Vol. 60, No. 9, 1970, pp. 1233–1236.

[13]Lee, S. C., "Dependent Scattering of an Obliquely Incident Plane Wave by a Collection of Parallel Cylinders," *Journal of Applied Physics*, Vol. 68, No. 10, 1990, pp. 4952–4957.

[14]Lee, S. C., "Scattering by Closely-Spaced Radially-Stratified Parallel Cylinders," *Journal of Quantitative Spectroscopy and Radiative Transfer*, Vol. 48, No. 2, 1992, pp. 119–130.

[15]Bose, S. K., and Mal, A. K. "Longitudinal Shear Waves in a Fiber-Reinforced Composite," *International Journal of Solid Structure*, Vol. 9, No. 9, 1973, pp. 1075–1085.

[16]Varadan, V. K., Varadan, V. V., and Pao, Y.-H, "Multiple Scattering of Elastic Waves by Cylinders of Arbitrary Cross Section. 1. SH Waves," *Journal of the Acoustical Society of America*, Vol. 63, No. 5, 1978, pp. 1310–1319.

[17]Lee, S. C., "Effective Propagation Constant of Fibrous Media Containing Parallel Fibers in the Dependent Scattering Regime," *Journal of Heat Transfer*, Vol. 114, No. 2, 1992, pp. 473–478.

[18]Lee, S. C., "Propagation of Radiation in High-Density Fibrous Composites Containing Coated Fibers," *Journal of Thermophysics and Heat Transfer*, Vol. 7, No. 4, 1993, pp. 637–643.

[19]White, S., and Kumar, S., "Interference Effects on Scattering by Parallel Fibers at Normal Incidence," *Journal of Thermophysics and Heat Transfer*, Vol. 4, No. 3, 1990, pp. 305–310.

[20]Kumar, S., and White, S., "Scattering Properties of Woven Fibrous Insulations: Effects of Interference for Normal Incidence," AIAA Paper 90-1674, June 1990.

[21]Lee, S. C., "Dependent Scattering by Parallel Fibers: Effects of Multiple Scattering and Wave Interference," *Journal of Thermophysics and Heat Transfer*, Vol. 6, No. 4, 1992, pp. 589–595.

[22]Twersky, V., "Propagation in Pair-Correlated Distributions of Small-Spaced Lossy Scatterers," *Journal of the Optical Society of America*, Vol. 69, No. 11, 1979, pp. 1567–1572.

[23]Wood, W. W., "Monte Carlo Calculations for Hard Disks in the Isothermal-Isobaric Ensemble," *Journal of Chemical Physics*, Vol. 44, No. 1, 1968, pp. 415–434.

[24]*User's Manual, IMSL Math/Library*, Vol. 2, Chap. 7, Version 1.1, Visual Numerics, Sugarland, TX, Inc., 1990.

[25]Kumar, S., "Thermal Radiation in Particulate Systems," Ph.D. Dissertation, Univ. of California, Berkeley, Berkeley, CA, 1987.